molecular pharmaceutics

ARTICLE

pubs.acs.org/molecularpharmaceutics

Effect of Structural Modification of α-Aminoxy Peptides on Their Intestinal Absorption and Transport Mechanism

Bin Ma,[†] Huiyan Zha,[‡] Na Li,[†] Dan Yang,[‡] and Ge Lin*[,†]

[†]School of Biomedical Sciences, The Chinese University of Hong Kong, Hong Kong SAR

[‡]Department of Chemistry, The University of Hong Kong, Hong Kong SAR

Supporting Information

ABSTRACT: A representative α-aminoxy peptide **1** has been demonstrated to have a potential for the treatment of human diseases associated with Cl^- channel dysfunctions. However, its poor intestinal absorption was determined. The purpose of this study was to delineate the transport mechanism responsible for its poor absorption and also to prepare peptide analogues by structural modifications of **1** at its isobutyl side chains without changing the α-aminoxy core for retaining biological activity to improve the intestinal absorption. The poor intestinal absorption of **1** was proved to be due to the P-glycoprotein (P-gp) mediated efflux transport in Caco-2 cell monolayer, intestinal segments in Ussing chamber and rat single pass intestinal perfusion models. Four analogues with propionic acid (**2**), butanamine (**3**), methyl (**4**) and hydroxymethyl side chains (**5**) were synthesized and tested using the same models. Except for the permeability of **2**, the absorbable permeability of the modified peptides in Caco-2 cell monolayer and their intestinal absorption in rats were significantly improved to 7-fold (**3**), 4-fold (**4**), 11-fold (**5**) and 36-fold (**2**), 42-fold (**3**), 55-fold (**4**), 102-fold (**5**), respectively, compared with **1** (P_{app}, 0.034 ± 0.003 × 10^{-6} cm/s; P_{blood}, 1.61 ± 0.807 × 10^{-6} cm/s). More interestingly, the structural modification remarkably altered transport mechanism of the peptides, leading to the conversion of the active transport via P-gp mediation (**1**, **2**), to MRP mediation (**3**), MRP plus BCRP mediation (**4**) or a passive diffusion (**5**). Furthermore, P-gp mediated efflux transport of **1** and **2** was demonstrated to not alter the P-gp expression, while **1** but not **2** exhibited uncompetitive inhibitory effect on P-gp ATPase. The results demonstrated that intestinal absorption and transport mechanism of the α-aminoxy peptides varied significantly with different structures, and their absorption can be dramatically improved by structural modifications, which allow us to further design and prepare better α-aminoxy peptide candidates with appropriate pharmacokinetic fates, including intestinal absorption, for potential clinical use.

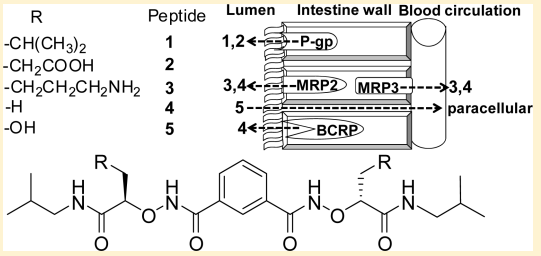

KEYWORDS: structural modification, absorption, transport mechanism, α-aminoxy peptide

INTRODUCTION

The diverse and important functions of peptides, including neurotransmitters, hormones, immunomodulators and enzyme inhibitors, increasingly attract more attentions to their investigation for clinical use. However, several properties of peptides, such as conformational flexibility, poor absorbability, rapid enzymatic degradation and low bioavailability, limit their potential as therapeutic agents. Therefore, structural modifications of the natural peptides to improve their function and bioavailability have become one of the focuses on peptide research in the recent decade. Among various classes of synthetic peptides, peptidomimetics, the small molecules mimicking the functions of natural peptides, have been developed and proved to have better metabolic stability and bioavailability.[1−3] Recently, our research team has started investigation of α-aminoxy peptides, a novel class of peptidomimetics, because they are analogues of *β*-peptides in which the *β*-carbon atom is replaced by an oxygen atom and have excellent metabolic stability toward proteases.[4−6] We have synthesized a series of α-aminoxy peptides and demonstrated that these α-aminoxy peptides formed predictable and backbone-controlled secondary structures.[3,7−9] It was revealed that α-aminoxy peptides self-assembled into synthetic ion channels in the lipid membranes and mediated ion flow across the membranes of living cells with remarkably high efficiency independent of natural chloride channels.[3,7−9] Our prototype α-aminoxy peptide **1** (Figure 1) was proven to form ion channels with a remarkable preference for Cl^- relative to other anions, such as Br^-, I^-, NO_3^- and $H_2PO_4^-$.[7] Hence, these novel synthetic α-aminoxy peptides have become lead compounds for further development to be potential drugs for the treatment of human diseases associated with Cl^- channel dysfunctions, such as cystic fibrosis, inherited kidney stone diseases, myotonia, and epilepsy.

As α-aminoxy peptides are novel candidates, their pharmacokinetics has not been studied. With the consideration of poor absorbability and rapid enzymatic degradation in the intestine as

Received: November 11, 2010
Accepted: June 1, 2011
Revised: May 9, 2011
Published: June 01, 2011

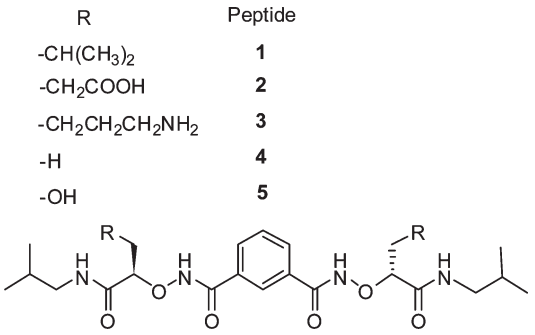

Figure 1. Chemical structures of five α-aminoxy peptides.

the common feature of natural peptides, the investigation of the absorption, transport mechanism, and metabolic stability of **1** in the intestine appeared to be our first task and therefore the primary aim of the present study. Our preliminary data of **1** indicated significantly low intestinal permeability due to the P-glycoprotein (P-gp) transporter-mediated efflux transport, thus four structurally modified α-aminoxy peptides (**2**−**5**, Figure 1) were synthesized to improve their intestinal absorption, and their activity of Cl^- ion channel formation was examined to be all positive (data will be reported in a separate paper).

The present study reports the structural modification of the representative α-aminoxy peptide **1** to yield four analogues (**2**−**5**), and the investigations of intestinal permeability of these peptides in Caco-2 cell monolayer and in intestinal segments as well as their intestinal absorption in rat model. In addition, the transport mechanisms of these peptides were delineated by inhibitory tests using different transporter inhibitors, and the potential interactions of peptides **1** and **2** with P-gp were further studied by Western blot and P-gp ATPase assay. The present study demonstrated significant improvements of intestinal absorption of α-aminoxy peptides and dramatic alteration of transport mechanisms by structural modification.

EXPERIMENTAL SECTION

Peptide Synthesis. Peptide **1** was synthesized by using our reported procedure.[7] The detailed synthetic process of four modified peptides and data for their structural elucidation are shown in the Supporting Information (SI1−SI12). The purity of all five peptides determined by HPLC−UV analysis is shown in the Supporting Information (SI13).

HPLC−UV and HPLC−MS Analysis. All samples tested in different models for peptides **2**−**5** were analyzed by HPLC−UV using an Agilent 1100 series LC system coupled with an autosampler (kept at 4 °C throughout the analysis) and a diode array detector (DAD). Separation of individual peptides and the corresponding internal standards were achieved using a Zorbax SB C_{18} column (150 mm × 4.6 mm i.d., 5 μm; Agilent, USA) with an Agilent C_{18} guard column (10 mm × 4.6 mm i.d., 5 μm) at 25 °C with a detecting wavelength at 230 nm. Detailed information on the mobile phase and internal standard for individual analytes is presented in the Supporting Information (SI14).

The analysis of samples for **1** tested in different models required a more sensitive HPLC−MS method and was performed using Perkin-Elmer PE-200 HPLC system (Perkin-Elmer, USA) connecting with an API 2000 Q-Trap mass spectrometer (AB Sciex, USA). The mass spectrometer was operated in positive ion mode using an ionspray interface with the following working parameters: ion spray voltage, 5500 V; curtain gas, 20 psi; gas 1, 40 psi; gas 2, 20 psi; source temperature, 400 °C. All gases used were nitrogen. Declustering potential was set at 106 and 86 V for **1** and ketoconazole (internal standard, IS), respectively. Entrance potential was set at 8.5 and 10 V for **1** and its IS, respectively. Multiple reaction monitoring (MRM) was employed for data acquisition. The optimal MRM fragmentation transitions were m/z 535.5 → m/z 145.9 with collision energy (CE) of 51 eV for **1** and m/z 531.3 → m/z 112.3 with CE of 57 eV for ketoconazole. The dwell time for each transition was 150 ms.

Cell Culture. Caco-2 cells from the American Type Culture Collection (Rockville, MD, USA) were cultured following the condition as described previously.[10] The harvested cells (39−46 passages) were plated onto six-well plates with Transwell inserts (24 mm i.d., 0.4 μm pore size, 4.67 cm^2 of growth area, polyester membrane, Corning Costar Co., NY) at a density of 3×10^5 cells/well and cultured for 21 days prior to transport experiments. The integrity of the monolayer was monitored by measuring the transepithelial electrical resistance (TEER) at 37 °C with an epithelial voltohmmeter (World Precision Instruments, Inc., USA). Two marker compounds, propranolol (transcellular marker) and atenolol (paracellular marker), were also subjected to the same conditions to test the integrity and function of the cell membrane. Only Caco-2 monolayer with TEER above 600 Ω·cm^2 or 450 Ω·cm^2 (after subtracting the background value of the Transwell) prior to or after transport experiment, and the P_{app} values of the marker compounds between the normal values were employed in the transport study (Supporting Information, SI15).[11,12]

Animals. Male Sprague−Dawley (SD) rats (280−320 g) were supplied by the Laboratory Animal Service Center, The Chinese University of Hong Kong. The rats were housed under standard conditions of temperature, humidity, and light. Food and water were provided *ad libitum*. The animal procedures and experiments were performed in accordance with the basic principles and guidelines of The Chinese University of Hong Kong for investigators conducting biomedical research involving animals.

***In Vitro* Permeability Study.** The transport study was carried out in HBSS supplemented with 10 mM HEPES transport buffer solution (pH 7.4). The stability of the peptides in the transport buffer was examined, and they proved to be stable (Supporting Information, SI16). The Caco-2 cell monolayer was rinsed twice and equilibrated with transport buffer at 37 °C for 15 min before the experiment. In the bidirectional transport study, the peptides (70 μM for **1**, 150 μM for **2**, 300 μM for **3**, 200 μM for **4** and **5**) were loaded onto the donor side, which was the apical (1.5 mL transport buffer) or basoleteral (2.6 mL of transport buffer) side corresponding to test the absorbable or secretory permeability, respectively, and incubated at 37 °C for 120 min. The concentrations used for individual peptides were chosen based on the corresponding limitation of the quantitative measurement in HPLC analysis. During the experiment, aliquot samples (0.4 mL) were taken from the receiver side, the other side from the loading side, at designed time intervals (0, 15, 30, 45, 60, 90, 120 min). A same volume of blank buffer was replaced to the receiver chamber after each sampling, and the resultant dilution factor was considered for the calculation of P_{app} value for each sampling. The collected samples were immediately mixed with 100 μL of methanol and stored at 4 °C until the analysis. In addition, an inhibitory study was performed to investigate the transport mechanisms of the peptides. Four P-gp inhibitors, namely, verapamil (25−150 μM), cyclosporin A (5 μM), TPGS (0.005%, w/v) and

Cr-EL (0.005%, w/v); two MRP inhibitors, probenecid (1 mM) and MK-571 (20 μM alone or 40 μM in combination with Ko 143); and two BCRP inhibitors, FTC (5 μM) and Ko 143 (5 μM), were used. After preincubation of each individual inhibitor in both sides for 15 min, the inhibitory transport study was performed using the same protocol of bidirectional transport described above. Furthermore, to determine the potential paracellular diffusion transport mechanism of **5**, the same bidirectional transport study using transport buffer with or without Ca^{2+} was performed.

***Ex Vivo* Animal Permeability Study.** Following the sacrifice of rats, segments of duodenum, jejunum and ileum were excised, washed, and kept in cold oxygenated (95% O_2/5% CO_2) Krebs–Henseleit buffer. The underlying muscularis was removed from the serosal side of the tissue before mounting. Each chamber was filled with 5 mL of Krebs–Henseleit buffer (37 °C, pH 7.4) with continuous lavaging of 95% O_2/5% CO_2 at a flow rate of approximately 50 ± 10 mL/min throughout the experiment. The resistance of tissue, which monitors the tissue viability, was determined by the measurement of potential differences at three current values (−5, 0, 5 μA) using EVC 4000 Precision V/I Clamp (World Precision Instruments, Inc., USA). Individual segments with resistance between 25 and 45 $\Omega \cdot cm^2$ after 30 min equilibration were selected for the intestinal absorption study. **1** (70 μM) or **2** (150 μM) was loaded into the donor chamber (mucosal side). The experiments continued for 90 min, and samples (1 mL) were withdrawn from the receiver chamber (serosal side) at designed time intervals (0, 30, 40, 50, 60, and 90 min). The sampled volume was replaced by blank buffer after each sampling. Similarly, the dilution factor was accounted for the calculation of P_{app} values. Each of the collected samples was mixed with 200 μL of methanol and stored at 4 °C until analysis. Similarly, P-gp inhibitor verapamil (100 μM) was used for the inhibitory study by preloading it into both chambers for 30 min followed by the same absorption protocol described above. The stability of **1** and **2** in Krebs–Henseleit buffer was investigated to be stable under the same experimental conditions (Supporting Information, SI17).

***In Situ* SPIP in Rats.** Prior to each experiment, the rats were fasted overnight (12–18 h) with free access to water. Before surgery, the rats were anesthetized with an intraperitoneal injection of 2 mL/kg of a solution containing 37.5 mg/mL ketamine and 5 mg/mL xylazine and placed on a heated surface maintained at 37 °C. The right jugular vein was cannulated for infusion of donor blood. Immediately after implanting the jugular vein cannula (0.4 mm i.d. × 0.8 mm o.d., SIMS Portex, U.K.), the abdomen was opened by midline incision of 3–4 cm. The entire small intestine was carefully exposed and cannulated on two ends with flexible PVC tubing (3 mm i.d. × 5 mm o.d.). The intestine was then flushed with prewarmed saline to remove intestinal contents. Mesenteric cannulation was performed using a Surflo iv catheter (0.8 mm × 51 mm, Terumo, Japan) for blood collection. Donor blood was infused through the right jugular vein using a peristaltic pump, and the rate was adjusted based on the outflow from the mesenteric blood (~0.4 mL/min). The *in situ* intestinal perfusions were initiated by infusing peptide containing solution (100 μM) from a 50 mL syringe (Hamilton Co., Reno, NV) at 0.5 mL/min. The blood from the mesenteric vein was continuously collected into heparinized tubes on ice and exchanged at 5 min intervals for 60 min. The blood samples were centrifuged at 6000*g* for 10 min, and the plasma was transferred to new tubes. An aliquot of 150 μL of plasma was mixed with 50 μL of corresponding IS solution, followed by addition of 280 μL of methanol. The mixture was vortexed and then centrifuged at 10000*g* for 5 min. A 50 μL aliquot of the supernatant was injected onto the HPLC system for analysis. Similarly, P-gp inhibitor Cr-EL (0.5%, w/v) was used for the inhibitory study by coperfusion with **1** followed by the same protocol described above. The stability of the peptides in rat plasma was studied under the same experimental conditions and proved to be all stable (Supporting Information, SI18).

The partition coefficient ($D_{RBC/P}$) between red blood cells (RBC) and plasma of individual peptides was determined. An aliquot of freshly drawn heparinized rat blood was transferred into Eppendorf tubes. An appropriate amount of the peptides was added to reach the final concentration at 2 and 10 μM, respectively. The blood samples were incubated at 37 °C for 60 min and then centrifuged at 6000*g* for 10 min. The generated plasma was transferred to new tubes, followed by addition of three volume of methanol. The mixture was vortexed and then centrifuged at 10000*g* for 5 min. A 50 μL aliquot of the supernatant was injected onto the HPLC system for analysis. In parallel, the same volume of blank blood was centrifuged to obtain the plasma. The same amount of individual peptides was added into the plasma and vortexed, and the samples were prepared and analyzed as described above. The RBC partitioning ratio was calculated by comparing the chromatographic peak areas of plasma samples obtained from the different preparation process. The results demonstrated that partition of **3** to RBC was about 13%, while the other four peptides showed no binding to RBC (Supporting Information, SI19).

Luminescent P-gp ATPase Assay. P-gp ATPase activity was estimated by P-gp-Glo assay system (Promega Corporation, Madison, WI, USA). The assay relies on the ATP dependence of the light-generating reaction of firefly luciferase. ATP consumption is detected as a decrease in luminescence. In a 96-well plate, recombinant human P-gp (25 μL) was incubated with verapamil (25 μM, control) or verapamil (25 μM) mixed with **1** or **2** (25 and 100 μM, respectively, tested samples). Verapamil serves as P-gp substrate, which stimulates the activity of ATPase for the consumption of ATP by P-gp. Verapamil-stimulated ATP consumption goes to a greater or lesser extent than the control, dependent on the effect of the test compound on ATPase. The reactions were initiated by adding 10 μL of 25 mM MgATP to all wells. The reaction was initiated by addition of MgATP (10 mM), stopped 40 min later by addition of 50 μL of firefly luciferase reaction mixture (ATP detection reagent) that initiated an ATP-dependent luminescence reaction. Signals were measured 20 min later by a Victor 1420 multilabel counter (EG&G Wallac, USA) and recorded as relative light units (RLU). The inhibitory mechanism of **1** on ATPase was investigated in the presence of various concentrations of **1** (50, 60, and 70 μM). The luminescence data were processed using a Lineweaver–Burk plot (or double reciprocal plot) to represent the ATPase kinetics. The reciprocal of ATPase activity, which was defined as the change in luminescence (RLU) over 40 min, in the presence of **1** was plotted against the reciprocal of substrate (verapamil) concentrations (35, 50, 65, 80, and 95 μM) to construct a regression line for each concentration group of **1**.

Western Blot Analysis of P-gp. Caco-2 cells were seeded at a density of 2 × 10^6 cells/dish in 60 mm dishes, and the medium was changed every other day. The cells were treated with DMEM containing **1** at 70 μM on day 18 for 72 h, and on day 20 for 24 h. Cells were harvested on day 21, and cellular protein was extracted with 150 μL of lysis buffer supplemented with protease inhibitors.

Protein extraction was conducted on ice to minimize any potential protein degradation. The mixture was then centrifuged at 15000*g* for 15 min at 4 °C. The supernatant containing the cell membrane proteins was subsequently transferred to new tubes, and the protein concentrations were measured using a Bio-Rad Protein Assay Kit (Bio-Rad Laboratories, Hercules, CA, USA) according to the manufacturer's instructions. Western blot for the immunodetection of P-gp was obtained using 60 μg of the extracted membrane proteins in loading buffer. Protein samples were separated on a 7.5% SDS−polyacrylamide and transferred onto a nitrocellulose membrane. The membrane was blocked by incubating for 1 h at room temperature with 5% nonfat milk in washing buffer, and then incubated overnight with the primary monoclonal antibody, C219 (1:1000, Covance Research Products, Dedham, MA). The membrane was washed (4 × 5 min), incubated with anti-mouse IgG horseradish peroxidase conjugate (1:3000, Thermo Scientific, Rockford, USA) for 1 h, washed again (4 × 5 min) and incubated with chemiluminescence detection reagent for 5 min. The protein was visualized by exposing the membrane to a ChemDoc XRS detection system (Bio-Rad, Milan, Italy). β-Actin served as internal standard, and it was similarly detected using a rabbit anti β-actin as primary antibody and anti-rabbit IgG as secondary antibody. Band intensity was analyzed, and P-gp expression was presented as the ratio of P-gp band intensity to β-actin band intensity in the same blot (P-gp/β-actin [%]).

Data Analysis. The P_{app} values of the peptides for Caco-2 cell monolayer and Ussing chamber model were calculated using the following equation:[13,14]

$$P_{app} = (dC/dt \times V)/AC_0$$

where dC/dt was the rate of the compound appearing in the receiver, which was determined from the slope of the linear regression of the measured receiver concentrations of compound vs time, V was the volume of the receiver chamber, A was the area of the membrane in the insert or area of the tissue in the chamber, and C_0 represented initial concentration of the compound in the donor chamber at 0 min.

Efflux ratio (ER) was calculated according to the following equation:

$$ER = P_{app(BtoA)}/P_{app(AtoB)}$$

In the SPIP model, the amount of the peptide in the blood was calculated as follows:

$$amount_B = con_P \times V_B \times 0.55 + D_{RBC/P} \times con_P \times V_B \times 0.45$$

where $amount_B$, con_P and V_B represent the amount of the peptide in the blood, plasma concentration of the peptide, and volume of the blood collected, respectively. $D_{RBC/P}$ was the partition coefficient of the peptide between red blood cells and plasma. Moreover, 0.45 is the reported Hematocrit value in rat.[15]

The P_{blood} value of the peptides absorbed into the mesenteric blood was calculated according to the following equation:[16,17]

$$P_{blood} = (dX/dt)/(2\pi rlC_0)$$

where dX/dt is the rate of the peptide appeared in mesenteric blood, r is the radius of the perfused intestine, which was reported to be 0.18 cm,[16,18] l is the length of the perfused intestine, and C_0 is the concentration of peptide in the perfusion solution.

Table 1. P_{app} Value of Five α-Aminoxy Peptides in Caco-2 Cell Monolayer Model

inhibitor	P_{app}[a] ($\times 10^{-6}$ cm/s) A to B	P_{app}[a] ($\times 10^{-6}$ cm/s) B to A
1		
no inhibitor	0.034 ± 0.003	3.80 ± 0.216
verapamil (100 μM)	1.04 ± 0.049***	3.00 ± 0.095***
cyclosporin A (5 μM)	0.737 ± 0.051***	3.45 ± 0.057*
TPGS (0.005%, w/v)	0.813 ± 0.164***	3.09 ± 0.150***
Cr-EL (0.005%, w/v)	0.477 ± 0.029***	2.36 ± 0.028***
2		
no inhibitor	0.019 ± 0.001	0.364 ± 0.021
verapamil (100 μM)	0.077 ± 0.030*	0.189 ± 0.036***
cyclosporin A (5 μM)	0.042 ± 0.010	0.156 ± 0.012***
3		
no inhibitor	0.241 ± 0.058	0.145 ± 0.011
probenecid (1 mM)	0.083 ± 0.008**	0.090 ± 0.006*
MK-571 (20 μM)	0.329 ± 0.010*	0.132 ± 0.032
4		
no inhibitor	0.123 ± 0.006	6.18 ± 0.211
probenecid (1 mM)	0.078 ± 0.005	3.57 ± 0.193***
MK-571 (20 μM)	0.222 ± 0.008*	4.24 ± 0.082***
FTC (5 μM)	0.148 ± 0.023	6.01 ± 0.303
Ko 143 (5 μM)	0.207 ± 0.011*	5.94 ± 0.312
MK-571 (40 μM) + Ko 143 (5 μM)	0.513 ± 0.076***	1.84 ± 0.117***
5		
no inhibitor	0.376 ± 0.018	0.661 ± 0.013

[a] $p < 0.05$, $p < 0.01$, and $p < 0.001$ compared with the corresponding control.

All data are presented as mean ± SD. One-way ANOVA followed by Bonferroni or Dunnett post test was used for multiple comparison as appropriate or two tailed unpaired *t*-test for two group comparison. A p value less than 0.05 was considered significant.

RESULTS

Synthesis. Peptide **1** was synthesized according to the procedure described before.[7] The four modified peptides were designed based on the structure of **1** to improve hydrophilic solubility by replacing the side chains of isobutyl in **1** with propionic acid for **2**, butanamine for **3**, methyl for **4** and hydroxymethyl for **5**, respectively. The detailed synthetic procedures and all characteristic data of the synthetic intermediates and designed products are provided in the Supporting Information (SI1−SI12). The purity of all designed peptides was determined to be all higher than 97% by HPLC−UV analysis and is also shown in the Supporting Information (SI13).

Permeability and Transport Mechanism in Caco-2 Cell Monolayer. Permeability coefficients (P_{app}) obtained from all five peptides tested in Caco-2 cell monolayer model are summarized in Table 1. The absorbable permeability coefficient ($P_{app\ (AtoB)}$) of **1** obtained from the apical (A) to the basoleteral (B) side was 0.034 ± 0.003 × 10^{-6} cm/s, indicating its very poor absorbability according to the generally acceptable $P_{app(AtoB)}$

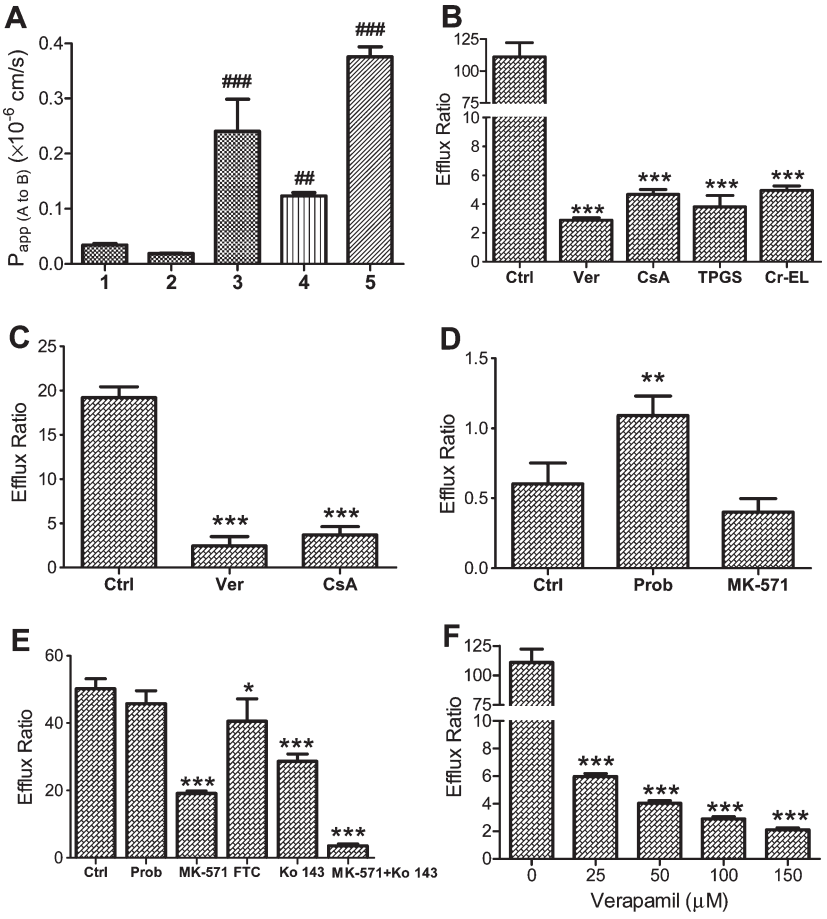

Figure 2. The $P_{app(AtoB)}$ values of the five peptides (A); efflux ratio of **1** (B), **2** (C), **3** (D), and **4** (E); efflux ratio of **1** at different concentrations of verapamil (F). Ctrl, control without inhibitor; Ver, verapamil; CsA, cyclosporin A; Prob, probenecid. $^{\#\#}p < 0.01$ and $^{\#\#\#}p < 0.001$ compared with **1**; $^{*}p < 0.05$ and $^{***}p < 0.001$ compared with the corresponding control group ($n = 3$).

value less than 1×10^{-6} cm/s for poor absorbable agents.[19] After structural modification, the absorbable permeability of the modified peptides was improved significantly in most of the cases (Figure 2A). Except for **2** ($P_{app(AtoB)}$: $0.019 \pm 0.001 \times 10^{-6}$ vs $0.034 \pm 0.003 \times 10^{-6}$ cm/s, $p = 0.504$), the absorbable permeability of the modified peptides significantly increased to about 4-fold (**4**), 7-fold (**3**) and 11-fold (**5**), respectively (Table 1). Although different concentrations of peptides were used in the present study due to their different limitations of quantitative measurement, the obtained P_{app} values were comparable among peptides, because their permeability was concentration-independent evidenced by the same P_{app} and efflux ratio values obtained at two different concentrations tested for the representative peptides **2** (150 and 300 μM) and **5** (200 and 500 μM) (data not shown). Furthermore, the concentrations for all peptides utilized did not saturate the corresponding efflux transporter(s) involved based on the evidence of a constant transport rate observed for all peptides within 120 min.

To further understand the reasons for the poor absorption of **1**, its transport mechanism was investigated. The secretory permeability coefficient ($P_{app(BtoA)}$) of **1** obtained from the basoleteral (B) to the apical (A) side was measured, and the efflux ratio (ER), which was calculated by the ratio of $P_{app(BtoA)}/P_{app(AtoB)}$ and utilized for the prediction of potential involvement of active efflux transport, was determined. A remarkably high ER value (112) of **1** was obtained (Figure 2B), indicating that **1** permeated enterocyte membrane preferentially to the apical side by a significant efflux transporter-mediated process. Further inhibitory studies confirmed that **1** was a substrate of P-gp and its poor absorbability was due to the P-gp mediated efflux, because the ER value of **1** was significantly reduced (Figure 2B) while the $P_{app(AtoB)}$ value was significantly increased (Table 1) by all four different P-gp inhibitors, namely, verapamil, cyclosporin A, D-α-tocopherol polyethylene glycol 1000 succinate (TPGS) and Cremophor-EL (Cr-EL). Furthermore, the inhibitory effect of verapamil on P-gp-mediated efflux was dose-dependent (Figure 2F).

Subsequently, the transport mechanisms of four modified peptides were investigated. The results demonstrated that transport of **2** was also mediated by P-gp but to a significantly less extent compared with **1** (ER: 19 vs 112), and such active transport was inhibited by both verapamil and cyclosporin A (Figure 2C). For peptide **3**, the ER value was about 0.6, suggesting its active transport mechanism favorable intestinal absorption from the apical to basoleteral side. Probenecid, a nonselective MRP inhibitor, significantly decreased permeability of **3** toward both directions and abolished the transporter-mediated active process to yield an ER value close to 1 (Table 1, Figure 2D), whereas MK-571, an MRP inhibitor with a relative selectivity toward MRP2, significantly increased its absorbable permeability but did not alter the ER. The results suggested that **3** was a substrate of different types of MRP transporters. In the case of **4**, the ER value of 50 demonstrated the involvement of active transporters. The ER

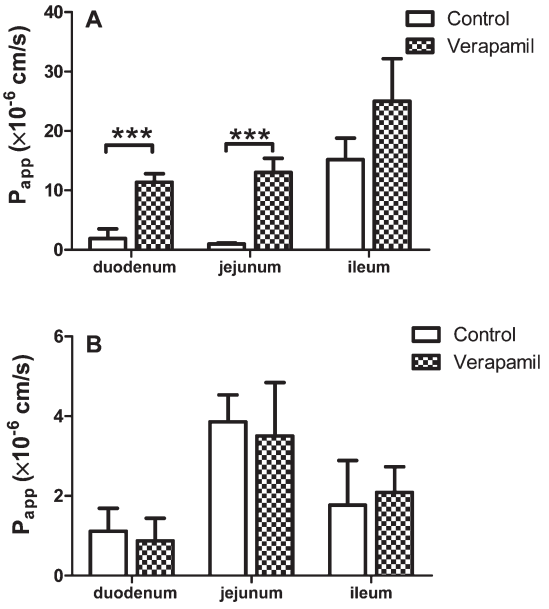

Figure 3. P_{app} values of **1** (A) and **2** (B) determined in duodenum, jejunum and ileum in the absence (control) and presence of verapamil in the Ussing chamber model. $^{***}p < 0.001$ compared with control ($n = 4$).

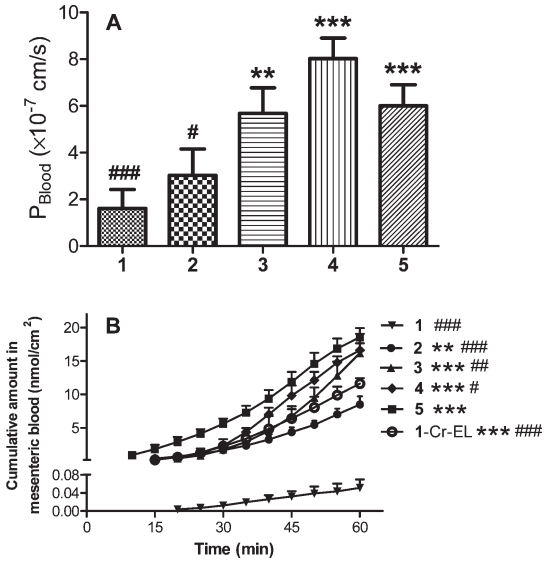

Figure 4. Absorption of five α-aminoxy peptides in rat SPIP model. P_{blood} values of the peptides (A) and cumulative amount in the mesenteric blood within 60 min (B). $^{**}p < 0.01$ and $^{***}p < 0.001$ compared with **1**; $^{\#}p < 0.05$, $^{\#\#}p < 0.01$ and $^{\#\#\#}p < 0.001$ compared with **5** ($n = 3$).

and/or $P_{app(BtoA)}$ values were reduced by either MRP inhibitors such as probenecid and MK-571 or BCRP inhibitors such as fumitremorgin C (FTC) and Ko 143. Moreover, in the presence of both MRP and BCRP inhibitors, the transporter-mediated active processes of **4** were nearly abolished (Table 1, Figure 2E). The results demonstrated that **4** was a substrate of both MRP and BCRP transporters. On the other hand, very similar P_{app} values of **5** were observed for both directions of transport (Table 1), and both efflux ratio and P_{app} values did not significantly change in the presence of different transporter inhibitors (data not shown), indicating that it penetrated the cell membrane without the involvement of any transporters. Compared with the results in the presence of Ca^{2+}, permeabilities of **5** were significantly increased in the absence of Ca^{2+} in both directions ($P_{app(AtoB)}$, $4.93 \pm 0.634 \times 10^{-6}$ vs $0.376 \pm 0.018 \times 10^{-6}$ cm/s, $p < 0.001$; $P_{app(BtoA)}$, $5.66 \pm 0.266 \times 10^{-6}$ vs $0.661 \pm 0.013 \times 10^{-6}$ cm/s, $p < 0.001$), further demonstrating that **5** transported paracellularly across the cell membrane. Moreover, the $P_{app(AtoB)}$ value of **5** was comparable to that (0.254×10^{-6} cm/s) of atenolol, a marker compound for paracellular diffusion, tested in parallel (Supporting Information SI15) and also to the generally accepted value for paracellular diffusion.[11,19,20] All the available data revealed that **5** was absorbed mainly through passive paracellular diffusion.

Absorption in Intestinal Segments. The effect of P-gp-mediated efflux on the absorption of **1** and **2** was further assessed in rat small intestinal segments in the Ussing chamber model. As shown in Figure 3A, absorption of **1** in duodenum and jejunum but not in ileum was significantly enhanced in the presence of verapamil (100 μM), indicating that P-gp-mediated efflux mainly reduced the absorption of **1** in duodenum and jejunum, whereas verapamil did not significantly alter absorbable permeability of **2** in all segments tested (Figure 3B), suggesting that although **2** was a P-gp substrate, its overall absorption in the small intestine was not significantly affected by P-gp-mediated efflux. This finding was also consistent with the results of the significantly less P-gp influence found in Caco-2 cell model.

Absorption in Live Animal. The intestinal absorption of five peptides was further investigated in the live animal using the *in situ* rat single pass intestinal perfusion model. The accumulated amounts of peptides in mesenteric blood within 60 min were determined (Figure 4). Furthermore, the *in vivo* permeability coefficient (P_{blood}) (Figure 4) was calculated based on the equation with the assumption of a constant concentration of peptide along the entire intestine, and considered as an additional estimated value for the comparison. Both P_{blood} value and accumulated amount of **1** were significantly lower than those of **3**, **4** and **5**, which is in good agreement with the results obtained *in vitro*. The accumulated amount of **1** in mesenteric blood was significantly enhanced by coperfusion with P-gp inhibitor Cr-EL (Figure 4B), which further confirmed the remarkable effect of P-gp on the intestinal absorption of **1** leading to its poor absorbability. Similar to the *in vitro* findings, the P_{blood} value of **2** was also similar to that of **1** but significantly lower than that of the other three peptides. However, the accumulated amount of **2** in mesenteric blood within 60 min was significantly higher than that of **1**. The results obtained *in vivo* also revealed that the effect of P-gp mediated efflux on the overall intestinal absorption of **2** was not remarkable and thus its amount absorbed into the bloodstream significantly increased to about 36-fold compared with **1**. Furthermore, compared with the limited amount of **1** absorbed within 60 min, after structural modification the absorbed amount of these peptides dramatically increased to approximately 42-fold (**3**), 55-fold (**4**) and 102-fold (**5**), respectively. The results further demonstrated that the intestinal absorption of **5** was the highest and significantly greater than that of the other four peptides tested (Figure 4B).

Interaction of Peptides with P-gp. The interaction of **1** and **2** with P-gp was further evaluated using ATPase assay in which the luminescent signal increased along with the decrease in ATP consumed by ATPase in the presence of verapamil, which acted as a substrate of P-gp to stimulate ATPase. Decrease in the consumption of ATP corresponds to the reduction of activity of ATPase and thus the inhibition of P-gp. As shown in Figure 5A, **1** dose-dependently

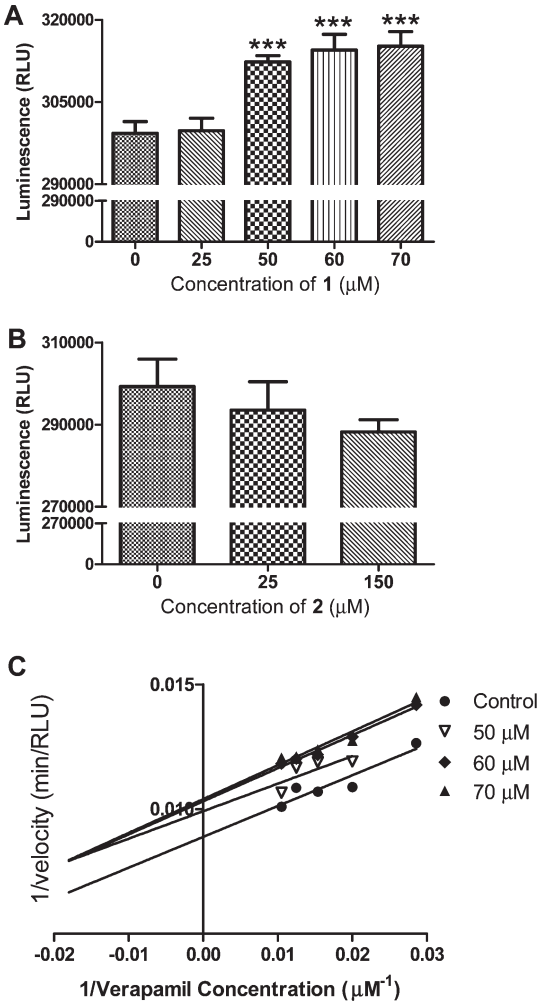

Figure 5. Interaction of **1** and **2** with P-gp ATPase. Inhibitory effect of **1** (A) and **2** (B) on P-gp ATPase, and inhibitory mechanism of **1** (C). ***$p < 0.001$ compared with control (absence of the peptides) ($n = 4$).

inhibited P-gp by the evidence of increase in luminescence signals, while peptide **2**, the other P-gp substrate, showed no significant inhibition of P-gp even at the highest concentration (150 μM) tested (Figure 5B).

The mechanism of P-gp inhibition was assessed using a Lineweaver−Burk plot[21] (Figure 5C). The results showed a parallel profile with different concentrations of **1**, indicating that the inhibition of P-gp by **1** was uncompetitive. Furthermore, Western blot assay demonstrated that **1** at 70 μM, which remarkably exhibited P-gp inhibition in ATPase assay, did not significantly affect the expression of P-gp in Caco-2 cells after incubation for 24 and 72 h (Figure 6).

■ DISCUSSION

Poor intestinal absorbability of **1** was revealed in all cell, organ and animal models tested. Since the metabolic instability in the intestine is one of the general factors leading to low absorption of natural peptides, such a factor was examined in the present study. Individual samples obtained from all three models were all analyzed by HPLC−MS, and no metabolites of **1** were detected. In addition, typical recoveries of **1** in Caco-2 and Ussing chamber models were determined to be 93.6 ± 1.97% and 96.3 ± 1.24%, respectively. The results confirmed that **1** was metabolically stable during the intestinal absorption. Subsequently, poor absorption of **1** found in all models tested was proven mainly due to the P-gp-mediated efflux transport, which facilitated the movement of **1** toward lumen and thus acted as a barrier to prevent its intestinal absorption.[22,23] Furthermore, the results demonstrated that **1** was a substrate of P-gp and uncompetitively inhibited P-gp via inhibition of the activity of ATPase without affecting P-gp expression.

In order to improve the intestinal absorption of **1**, the structural modification was conducted to synthesize four analogues. Our strategy was to alter the potential binding sites of **1** in order to circumvent the P-gp-mediated efflux transport and also to keep a minimum change in the core α-aminoxy peptide moiety in order to retain its biological activity and metabolic stability. Thus, structural modification was focused on isobutyl side chains of **1**. Although numerous molecules with diverse structures have been found as P-gp substrates, it has been reported that neutral and hydrophobic compounds tended to be P-gp substrates, while a charged residue in the structure appeared to be able to eliminate the stimulatory effect of P-gp ATPase activity and consequently less affected by P-gp.[22,24,25] Therefore, α-aminoxy peptides **2** and **3** were designed to be negatively and positively charged molecules at physiological pH and were synthesized by replacement of isobutyl groups in **1** with propionic acid and butanamine, respectively (Figure 1). Although **2** was also evidenced as a substrate of P-gp with an ER value of 19 in the cell model but with no inhibitory effect on P-gp, its ER value was significantly decreased by 6-fold comparing with **1**. Moreover, P-gp was proven not playing a significant role in the absorption of **2** in the intestinal segments and its amount absorbed into bloodstream was remarkably improved by 36-fold compared with **1** in the animal model. The results demonstrated that **2** as an α-aminoxy peptide anion at physiological pH significantly reduced, if it did not abolish, the influence of P-gp-mediated efflux transport and thus improved the intestinal absorption dramatically.

On the other hand, in the case of **3**, an α-aminoxy peptide cation under physiological conditions, its ER value was less than 1, suggesting the active transport mechanism favorable to absorption. Compared with **1**, its absorbable permeability in Caco-2 cells and intestinal absorption in rats significantly increased to 7-fold and 42-fold, respectively. The mechanism study revealed that **3** became a substrate of MRP. It is well-known that different types of MRP transporters locate at different sides of enterocyte membrane, for instance, MRP2 mainly expresses on the apical side and MRP3 on the basoleteral side to facilitate efflux toward lumen and bloodstream, respectively.[26,27] The nonselective MRP inhibitor probenecid significantly inhibited both absorbable and secretory P_{app} values of **3** (Table 1) and brought the ER back to 1, while MK-571, which was reported to inhibit various types of MRP and has a relative selectivity toward MRP2,[28,29] significantly enhanced the absorbable permeability but did not alter the ER of **3** (Table 1, Figure 2D). The results demonstrated that **3** was a substrate of different types of MRP with a preference for those mediating efflux toward bloodstream. However, which type of MRP plays the major role in the transport of **3** is unknown and needs to be further investigated. Nevertheless, comparing with **1** and **2**, the intestinal absorption of **3** was improved significantly as evidenced in the cell and animal models investigated. The results demonstrated that the structural modification to produce **3** successfully achieved our goals of the improvement of absorption and circumvention of the P-gp-mediated efflux transport.

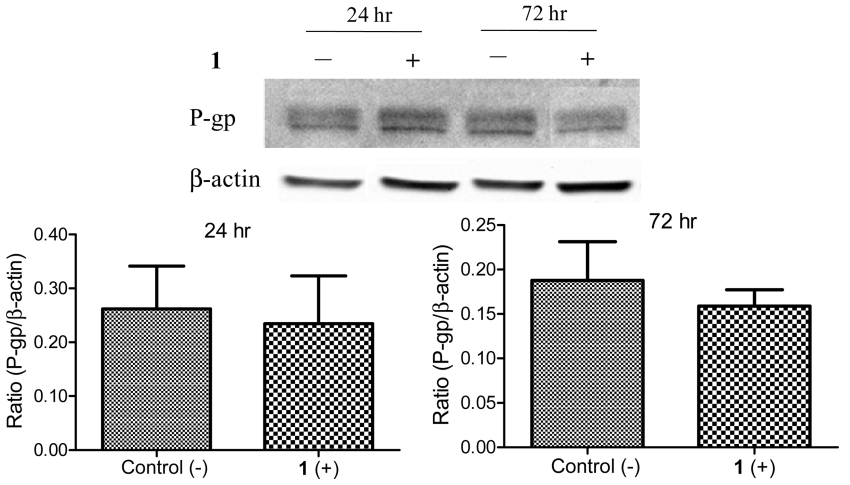

Figure 6. Effect of **1** on the expression of P-gp in Caco-2 cells tested by Western blot (representative of three independent experiments).

However, the study could not be stopped at this stage because of the emergence of a new transport mechanism of **3** mediated by MRP. Subsequently, using the same strategy, further structural modification was performed by decreasing the length of the isobutyl side chains of **1** to prepare **4** by the replacement with methyl group and **5** with hydroxymethyl group (Figure 1). Again, the absorbable permeability and intestinal absorption of **4** were significantly improved compared with **1**, and its overall absorption was also comparable to that of **3** (Figure 4). The results obtained from the mechanism study indicated that **4** was a substrate of both MRP and BCRP transporters. With the consideration of different types of MRP, MRP2 appeared to play an important role because only the selective (MK-571) rather than the nonselective (probenecid) MRP inhibitor significantly decreased the ER value. Moreover, MK-571 together with Ko 143 (BCRP inhibitor) was able to abolish all transporter-mediated active transport (Figure 2E). These findings demonstrated that a slight alteration of the side chains of these peptides led to remarkable changes of the transport mechanisms in that the active transport with P-gp mediation for **1** was converted to MRP mediation for **3** or both MRP and BCRP mediation for **4**.

Peptide **5** exhibited the best absorbability among all five peptides tested. More importantly and interestingly, efflux transporters were no longer involved in the transport of **5**, and thus **5** crossed the enterocyte membrane by passive diffusion along with concentration gradient. Furthermore, its intestinal permeability ($P_{app(AtoB)}$, $0.376 \pm 0.018 \times 10^{-6}$ cm/s), which is comparable to the generally accepted value for paracellular diffusion (through the tight junction between the enterocyte cells),[11,19,20] demonstrated that **5** was absorbed from the intestine by passive diffusion mainly via the paracellular pathway. The paracellular transport was further confirmed using a well-established method by removal of Ca^{2+} from the transport buffer to disrupt tight junctions in Caco-2 monolayer.[30−32] The results revealed that in the absence of Ca^{2+} the transport of **5** was significantly enhanced by 13- and 15-fold in both the A to B and B to A directions. The paracellular absorption mechanism has also been reported for several known peptide drugs, such as octreotide,[33] vasopressin[34] and salmon calcitonin.[35] One possible explanation for the absence of active transport of **5** was that, due to the structural modification with introducing hydroxymethyl group in the side chain, an intramolecular hydrogen bond might form, which would alter the binding site of the peptide to transporters and interrupt the interaction between the peptide and transporters.[36] Based on the results obtained from all five peptides tested, the side chains of isobutane in **1**, propionic acid in **2**, butanamine in **3** and methyl in **4** are suggested to be their binding sites interacting with the corresponding transporters, while such binding sites vanished in **5**. Further in-depth study to verify the specific biding sites of individual peptides is warranted. It is noted that there was no obvious correlation between log *P* values (**1**, 4.31; **2**, 0.84; **3**, 1.32; **4**, 1.84; **5**, 0.13, estimated using ChemDraw Ultra 10.0, CambridgeSoft Corporation, MA, USA) and permeation behavior of the peptides, further indicating the important role of active efflux transporter-mediated mechanism in the transport of these peptides, especially peptides **1**−**4**. The present study proved the significant role of various efflux transporters in the intestinal absorption of four of five α-aminoxy peptides examined, however, whether the uptake transporters, especially those mediating the absorption of naturally occurring short di- and tripeptides, such as OATP and PEPT1,[37,38] are also involved in the absorption of the synthetic α-aminoxy peptides is unknown and warranted for further investigations.

Table 2. Transport Mechanism of Five α-Aminoxy Peptides

peptide	transport mechanism
1	significant P-gp-mediated active transport
2	P-gp-mediated active transport
3	MRP-mediated active transport
4	BCRP and MRP-mediated active transport
5	passive diffusion via paracellular pathway

In addition to the structural modification, our results also demonstrated that coadministration of P-gp inhibitors might be another alternative approach to improve intestinal absorption of **1**. Various pharmaceutical excipients, including TPGS and Cr-EL tested in the present study, are P-gp inhibitors but have minimal or no pharmacological activity.[24,39] Our results demonstrated that both TPGS and Cr-EL also significantly enhanced intestinal absorption of **1**. Using such pharmaceutical excipients will be more appropriate than P-gp inhibitors, such as verapamil and cyclosporin A commonly utilized in the transport mechanism study, because these P-gp inhibitors have their own pharmacological

activities and may cause unwanted adverse effects when concurrently administered with the P-gp substrate.

CONCLUSIONS

The intestinal absorption of α-aminoxy peptide **1** was demonstrated to be poor due to a significant efflux transport mediated by P-gp. In order to improve the absorption of **1**, structural modifications in particular in its isobutyl side chains were designed to produce four peptide analogues **2**−**5**. The results revealed that, with slight alterations of isobutyl side chains, the intestinal absorption of **1** has been significantly improved to 36-fold for **2**, 42-fold for **3**, 55-fold for **4** and 102-fold for **5**, respectively. Furthermore, such structural modification dramatically altered transport mechanism of the peptides with the conversion of the active transport via P-gp mediation (**1**, **2**), to MRP mediation (**3**), MRP plus BCRP mediation (**4**) or even a passive diffusion (**5**) (Table 2), suggesting that isobutyl side chains in **1** and the modified side chains in **2**−**4** might be the binding sites of individual peptides interacting with different transporters, while the function of such binding sites was abolished in **5** as evidenced by its passive diffusion without the involvement of any efflux transporters. Our findings provided scientific evidence and rationale for further design and development of better α-aminoxy peptide candidates with improved intestinal absorption for potential clinical use.

ASSOCIATED CONTENT

Supporting Information. Additional information as noted in the text, including the synthesis and structural identification of four modified α-aminoxy peptides, purity test of all five peptides by HPLC−UV, mobile phase for the analysis of all peptides, absorption of marker compounds in Caco-2 cell monolayer model, stability of the peptides in transport buffer, Krebs−Henseleit buffer, rat plasma under different conditions, and the results of binding test for the interaction of all peptides with red blood cells. This material is available free of charge via the Internet at http://pubs.acs.org.

AUTHOR INFORMATION

Corresponding Author

*Room 415, Basic Medical Sciences Building, The Chinese University of Hong Kong, Shatin, Hong Kong, China. Phone: +852-26096824. Fax: +852-26035139. E-mail: linge@cuhk.edu.hk.

ACKNOWLEDGMENT

This work was supported by Hong Kong RGC Central Allocation fund (HKU 2/06C).

ABBREVIATIONS USED

P-gp, P-glycoprotein; MRP, multidrug resistance-associated protein; BCRP, breast cancer resistance protein; ER, efflux ratio; SPIP, single-pass intestinal perfusion; TPGS, D-α-tocopherol polyethylene glycol 1000 succinate; Cr-EL, Cremophor-EL; FTC, fumitremorgin C; TEER, transepithelial electrical resistance; LC−MS, liquid chromatographic/tandem mass spectrometry; DAD, diode array detector; MRM, multiple reaction monitoring; DMEM, Dulbecco's modified Eagle's medium; HBSS, Hanks balanced salt solution; FBS, fetal bovine serum; P_{app}, permeability coefficient; RBC, red blood cells; RLU, relative light unit

REFERENCES

(1) Goodman, C. M.; Choi, S.; Shandler, S.; DeGrado, W. F. Foldamers as versatile frameworks for the design and evolution of function. *Nat. Chem. Biol.* **2007**, *3*, 252–262.

(2) Hill, D. J.; Mio, M. J.; Prince, R. B.; Hughes, T. S.; Moore, J. S. A field guide to foldamers. *Chem. Rev.* **2001**, *101*, 3893–4012.

(3) Li, X.; Wu, Y. D.; Yang, D. Alpha-aminoxy acids: new possibilities from foldamers to anion receptors and channels. *Acc. Chem. Res.* **2008**, *41*, 1428–1438.

(4) Wu, Y. D.; Wang, D. P.; Chan, K. W. K.; Yang, D. Theoretical study of peptides formed by aminoxy acids. *J. Am. Chem. Soc.* **1999**, *121*, 11189–11196.

(5) Frackenpohl, J.; Arvidsson, P. I.; Schreiber, J. V.; Seebach, D. The outstanding biological stability of beta- and gamma-peptides toward proteolytic enzymes: an in vitro investigation with fifteen peptidases. *ChemBioChem* **2001**, *2*, 445–455.

(6) Li, X.; Yang, D. Peptides of aminoxy acids as foldamers. *Chem. Commun. (Cambridge)* **2006**, *28*, 3367–3379.

(7) Li, X.; Shen, B.; Yao, X. Q.; Yang, D. A Small synthetic molecule forms chloride channels to mediate chloride transport across cell membranes. *J. Am. Chem. Soc.* **2007**, *129*, 7264–7265.

(8) Yang, D.; Li, X.; Sha, Y.; Wu, Y. D. A cyclic hexapeptide comprising alternating alpha-aminoxy and alpha-amino acids is a selective chloride ion receptor. *Chemistry* **2005**, *11*, 3005–3009.

(9) Yang, D.; Qu, J.; Li, W.; Zhang, Y. H.; Ren, Y.; Wang, D. P.; Wu, Y. D. Cyclic hexapeptide of D,L-alpha-aminoxy acids as a selective receptor for chloride ion. *J. Am. Chem. Soc.* **2002**, *124*, 12410–12411.

(10) Zhang, L.; Zheng, Y.; Chow, M. S.; Zuo, Z. Investigation of intestinal absorption and disposition of green tea catechins by Caco-2 monolayer model. *Int. J. Pharm.* **2004**, *287*, 1–12.

(11) Artursson, P. Epithelial transport of drugs in cell culture. I: A model for studying the passive diffusion of drugs over intestinal absorptive (Caco-2) cells. *J. Pharm. Sci.* **1990**, *79*, 476–482.

(12) Asano, T.; Ishihara, K.; Morota, T.; Takeda, S.; Aburada, M. Permeability of the flavonoids liquiritigenin and its glycosides in licorice roots and davidigenin, a hydrogenated metabolite of liquiritigenin, using human intestinal cell line Caco-2. *J. Ethnopharmacol.* **2003**, *89*, 285–289.

(13) Artursson, P.; Karlsson, J. Correlation between oral drug absorption in humans and apparent drug permeability coefficients in human intestinal epithelial (Caco-2) cells. *Biochem. Biophys. Res. Commun.* **1991**, *175*, 880–885.

(14) Sun, H.; Zhang, L.; Chow, E. C.; Lin, G.; Zuo, Z.; Pang, K. S. A catenary model to study transport and conjugation of baicalein, a bioactive flavonoid, in the Caco-2 cell monolayer: demonstration of substrate inhibition. *J Pharmacol Exp Ther.* **2008**, *326*, 117–126.

(15) Okudaira, N.; Tatebayashi, T.; Speirs, G. C.; Komiya, I.; Sugiyama, Y. A study of the intestinal absorption of an ester-type prodrug, ME3229, in rats: active efflux transport as a cause of poor bioavailability of the active drug. *J. Pharmacol. Exp. Ther.* **2000**, *294*, 580–587.

(16) Cummins, C. L.; Salphati, L.; Reid, M. J.; Benet, L. Z. In vivo modulation of intestinal CYP3A metabolism by P-glycoprotein: studies using the rat single-pass intestinal perfusion model. *J. Pharmacol. Exp. Ther.* **2003**, *305*, 306–314.

(17) Zhang, L.; Lin, G.; Chang, Q.; Zuo, Z. Role of intestinal first-pass metabolism of baicalein in its absorption process. *Pharm. Res.* **2005**, *22*, 1050–1058.

(18) Cook, T. J.; Shenoy, S. S. Intestinal permeability of chlorpyrifos using the single-pass intestinal perfusion method in the rat. *Toxicology* **2003**, *184*, 125–133.

(19) Yee, S. In vitro permeability across Caco-2 cells (colonic) can predict in vivo (small intestinal) absorption in man--fact or myth. *Pharm. Res.* **1997**, *14*, 763–766.

(20) Zhang, L.; Lin, G.; Kovacs, B.; Jani, M.; Krajcsi, P.; Zuo, Z. Mechanistic study on the intestinal absorption and disposition of baicalein. *Eur. J. Pharm. Sci.* **2007**, *31*, 221–231.

(21) Zhang, Z. Y.; Wong, Y. N. Enzyme kinetics for clinically relevant CYP inhibition. *Curr. Drug Metab.* **2005**, *6*, 241–257.

(22) Ambudkar, S. V.; Dey, S.; Hrycyna, C. A.; Ramachandra, M.; Pastan, I.; Gottesman, M. M. Biochemical, cellular, and pharmacological aspects of the multidrug transporter. *Annu. Rev. Pharmacol. Toxicol.* **1999**, *39*, 361–398.

(23) Zhang, L.; Zhang, Y. D.; Strong, J. M.; Reynolds, K. S.; Huang, S. M. A regulatory viewpoint on transporter-based drug interactions. *Xenobiotica* **2008**, *38*, 709–724.

(24) Constantinides, P. P.; Wasan, K. M. Lipid formulation strategies for enhancing intestinal transport and absorption of P-glycoprotein (P-gp) substrate drugs: in vitro/in vivo case studies. *J. Pharm. Sci.* **2007**, *96*, 235–248.

(25) MacLean, C.; Moenning, U.; Reichel, A.; Fricker, G. Closing the gaps: a full scan of the intestinal expression of p-glycoprotein, breast cancer resistance protein, and multidrug resistance-associated protein 2 in male and female rats. *Drug Metab. Pharmacokinet.* **2008**, *36*, 1249–1254.

(26) Bock-Hennig, B. S.; Kohle, C.; Nill, K.; Bock, K. W. Influence of t-butylhydroquinone and beta-naphthoflavone on formation and transport of 4-methylumbelliferone glucuronide in Caco-2/TC-7 cell monolayers. *Biochem. Pharmacol.* **2002**, *63*, 123–128.

(27) Prime-Chapman, H. M.; Fearn, R. A.; Cooper, A. E.; Moore, V.; Hirst, B. H. Differential multidrug resistance-associated protein 1 through 6 isoform expression and function in human intestinal epithelial Caco-2 cells. *J. Pharmacol. Exp. Ther.* **2004**, *311*, 476–484.

(28) Berger, V.; Gabriel, A. F.; Sergent, T.; Trouet, A.; Larondelle, Y.; Schneider, Y. J. Interaction of ochratoxin A with human intestinal Caco-2 cells: possible implication of a multidrug resistance-associated protein (MRP2). *Toxicol. Lett.* **2003**, *140−141*, 465–476.

(29) Schrickx, J.; Lektarau, Y.; Fink-Gremmels, J. Ochratoxin A secretion by ATP-dependent membrane transporters in Caco-2 cells. *Arch. Toxicol.* **2006**, *80*, 243–249.

(30) Artursson, P.; Magnusson, C. Epithelial transport of drugs in cell culture. II: Effect of extracellular calcium concentration on the paracellular transport of drugs of different lipophilicities across monolayers of intestinal epithelial (Caco-2) cells. *J. Pharm. Sci.* **1990**, *79*, 595–600.

(31) McMillan, J. M.; Walle, U. K.; Walle, T. S-adenosyl-L-methionine: transcellular transport and uptake by Caco-2 cells and hepatocytes. *J. Pharm. Pharmacol.* **2005**, *57*, 599–605.

(32) Stetinova, V.; Smetanova, L.; Kholova, D.; Svoboda, Z.; Kvetina, J. Transepithelial transport of ambroxol hydrochloride across human intestinal Caco-2 cell monolayers. *Gen. Physiol. Biophys.* **2009**, *28*, 309–315.

(33) Dorkoosh, F. A.; Broekhuizen, C. A.; Borchard, G.; Rafiee-Tehrani, M.; Verhoef, J. C.; Junginger, H. E. Transport of octreotide and evaluation of mechanism of opening the paracellular tight junctions using superporous hydrogel polymers in Caco-2 cell monolayers. *J. Pharm. Sci.* **2004**, *93*, 743–752.

(34) Hilgendorf, C.; Ahlin, G.; Seithel, A.; Artursson, P.; Ungell, A. L.; Karlsson, J. Expression of thirty-six drug transporter genes in human intestine, liver, kidney, and organotypic cell lines. *Drug Metab. Dispos.* **2007**, *35*, 1333–1340.

(35) Lee, Y. H.; Sinko, P. J. Oral delivery of salmon calcitonin. *Adv. Drug Delivery Rev.* **2000**, *42*, 225–238.

(36) Raub, T. J. P-glycoprotein recognition of substrates and circumvention through rational drug design. *Mol. Pharmaceutics* **2006**, *3*, 3–25.

(37) Giacomini, K. M.; Huang, S. M.; Tweedie, D. J.; Benet, L. Z.; Brouwer, K. L.; Chu, X.; Dahlin, A.; Evers, R.; Fischer, V.; Hillgren, K. M.; Hoffmaster, K. A.; Ishikawa, T.; Keppler, D.; Kim, R. B.; Lee, C. A.; Niemi, M.; Polli, J. W.; Sugiyama, Y.; Swaan, P. W.; Ware, J. A.; Wright, S. H.; Yee, S. W.; Zamek-Gliszczynski, M. J.; Zhang, L. Membrane transporters in drug development. *Nat. Rev. Drug Discovery* **2010**, *9*, 215–236.

(38) Klaassen, C. D.; Aleksunes, L. M. Xenobiotic, bile acid, and cholesterol transporters: function and regulation. *Pharmacol. Rev.* **2010**, *62*, 1–96.

(39) Honda, Y.; Ushigome, F.; Koyabu, N.; Morimoto, S.; Shoyama, Y.; Uchiumi, T.; Kuwano, M.; Ohtani, H.; Sawada, Y. Effects of grapefruit juice and orange juice components on P-glycoprotein- and MRP2-mediated drug efflux. *Br. J. Pharmacol.* **2004**, *143*, 856–864.